Hybrid Optimization of Star Grain Performance Prediction Tool

Anwer E. A. Hashish
MSc. Student
Anwar.hashish@mtc.edu.eg

Mahmoud Y.M. Ahmed
Associate Professor in Aerospace Engineering

Hamed M. Abdallah
Associate Professor in Aerospace Engineering

Mohamed A. Alsenbawy
Associate Professor in Aerospace Engineering
Aerospace Department – Military Technical College

ABSTRACT

In solid propellant rocket propulsion, the design of the propellant grain is a decisive aspect. The grain design governs the entire motor performance and, hence, the whole rocket mission. The ability to decide, during design phase, the proper grain design that satisfies the predefined rocket mission with minimum losses is the ultimate goal of solid propulsion experts. This study enables to predict the pressure time curve of rocket motor with star grain configuration and also to optimize the performance prediction tool through optimization methods to maximize its prediction efficiency. A hybrid optimization technique is used. Genetic Algorithm (GA) is first implemented to find the global optimum followed by Simulated Annealing (SA) optimization method to find the accurate local optimum. A program for predicting the pressure time curve of the rocket motor is created on MATLAB and then linked to GA - SA optimizers as an application on a case study. The purposed approach is validated against satisfying data. It is found that the developed optimized program is capable of predicting rocket motor performance (including the effect of erosive burning) with acceptable accuracy for preliminary design purposes.

KEYWORDS: *solid propellant propulsion, star grain, hybrid evolutionary optimization.*

NOMENCLATURE

Uppercase letters
A_p - Port area of star grain at each burning step
A^* - Critical section area of the nozzle,
A_b - burning area of the grain at each step
C^* - Propellant characteristic velocity
L_g - Length of star grain
M_n - Gas Mach number at the nozzle end of the grain
N - No of star points
P_{on} - Stagnation pressure of flowing gases
P_n - Pressure at nozzle end
P_h - Gas pressure at head end of the grain
R_{in} - Grain inner radius
RMSE - Root mean square error
P_D - discharge pressure
V_{cf} - Final chamber volume
V_n - flow velocity of gases at the nozzle end
V_{ci} - Initial volume of combustion chamber

Lowercase letters
a - Burning rate coefficient
d_{cr} - Initial critical diameter of nozzle
er_{rate} - Erosion rate of nozzle critical section
f - Fillet radius
j - Burning step
$\dot{m}_D$ - Rate of discharge of gases
$\dot{m}_G$ - Rate of generation of gases
n - Pressure exponent
r_h - Burning rate at the head end of the grain
r_n - Total burning rate at the nozzle end due to applying the erosive burning rate
r_{av} - Average burning rate of the grain
Δt - Time increment
t_{delay} - Delay time until begin of erosion
w - Web thickness
Δy - Distance burnt
Greek symbols

$\propto$ - Step regression factor
β - Head end regression factor
γ - Specific heat ratio of the combustion gases
ε - Angle fraction
ρ - Density of the burning propellant
θ - Star point angle
Γ - Specific gas constant

Subscripts
b – Burning
n – Nozzle
h – Head
i – Initial
f – Final
cr - Critical

1 INTRODUCTION

The solid propellant grain design involves numerous parameters that are commonly referred to as the grain ballistic parameters. These parameters can be classified into distinct categories as follows [1]:

- Properties of solid propellant, this category includes the following parameters: Total impulse, specific heat ratio, Propellant material, burning rate, characteristic velocity and propellant density.
- Mission requirements which include both thrust and thrust coefficient.
- Grain geometry: that includes web fraction, propellant geometric configuration, volumetric loading coefficient and slenderness ratio.
- Nozzle geometry, this category includes: exit area, throat area, nozzle shape, convergence and divergence angles and expansion ratio, erosion pattern of nozzle throat.
- Other ballistic parameters includes: combustion chamber material, weight and pressure, exit pressure, combustion temperature, burning time and motor diameter.

Clearly, the proper design of solid propellant rocket motors (SPRMs) involves multi-disciplinary algorithms to develop efficiently and accurately the designs related to the required performance parameters. Over the years, researchers developed tools for the preliminary design of SPRMs that can be optimized to the required performance criteria. Generally, these tools comprise three steps: geometric modeling, burn back analysis and optimization.
Many optimization objectives have been acquire through numerous optimization techniques.
One objective was to minimize the propellant mass. Nisar [2] used a hyprid optimization technique (genetic algorithm and sequential quadratic programming) on 3D finocyl grain involving 18 parameters. Similarly, Fredy [3] used GA on different grain geometries (end burning, tubular, star, etc.) which had up to 8 parameters. In contrast, Kamran[4] investigated different optimization objectives such as maximum volumetric loading fraction, minimum sliver fraction and maximum total impulse using GA on convex star grain with 6 parameters. In another study, Kamran [5] also used GA to find the maximum average thrust of 3D grain configuration with radial slots having 24 different parameters.
The research group of Raza et. al. conducted a series of studies on optimizing the dual thrust rocket motors (DTRMs). In these studies [6-9], the focus was to maximize the average boost-to-sustain thrust ratio and total impulse of DTRMs. They used different hybrid optimization techniques on different types of 3D grains. In [6], they used hybrid evolutionary GA and SA on 3D wagon wheel with 10 parameters. Similarly, in [7, 9] Raza et. al. used the same hybrid optimization technique on 3D finocyl grains (convex star tapered hollow cylinder grain geometry with 8 different design parameters and fin tapered hollow tubular with 8 design parameters). In contrast, in [8] they used a different hybrid optimization technique (SA and pattern search) on 3D finocyl grain with 8 parameters.
In all cases, researchers rely on theoretical techniques to predict the performance of SPRMs. The accuracy of such tools is a crucial aspect as far as credibility of these tools is concerned. This motivated many researchers to improve the accuracy of the tool they use via, in many cases, optimization. In this respect, the optimization technique is used to minimize the root mean square error (RMSE) between the desired and computed performance merit. In [10-13], different optimization methods were used such as complex method, pattern search and genetic algorithm. Sforzini [12] used pattern search for optimizing the computed thrust-time profile of a 3D finocyl grain with 10 parameters. Both Acik [11] and Yücel [10] used complex method to find the minimum RMSE but on different cases. Acik [11] optimized different grain geometries (end burning, internal burning tube, slot, slot-tube, star and star-tube) with parameters up to 9. Yücel [10] optimized a 3-D finocyl grain with 8 axial slots at the fore end and a radial slot at the aft end with 11 parameters. He also used genetic algorithm on his case study. Recently, Gawad [13] used genetic algorithm to find the minimum RMSE but on DTRM with tubular grain with two different diameters and sloped grain near its head end with 10 parameters.

It is clear that many studies implemented GA as the optimization method. This may be justified by its ability to define the global optimum inside the domain of study. For more accurate results, researchers refine optimization results via a hybrid optimization technique with a method for global search followed by a method using local search superiority.
The focus of the present study is to develop an optimized tool to predict the pressure time profile of a star grain. Acik [11] conducted a similar study, but using complex as the optimizer method. In this study, a different approach is adopted in which a hybrid GA-SA optimization is implemented.
The remainder of this paper is organized as follows. The next section presents the case study and the methodology of calculating pressure-time history followed by the optimization technique. The following section includes the results of this study. Conclusion and future work wrap up the paper.

2 CASE STUDY AND METHODOLOGY

2.1 Internal ballistics prediction model

A mathematical model for the internal ballistics of the solid propellant grain is developed based on the mass balance of the gas products [14, 15]. The developed model adopts the following assumptions:

- The flow of gases is adiabatic. The flow along the combustion chamber is isentropic.
- The gas products are ideal gases.
- Regression of surface along the grain length is linear.

The computations are performed in two sections; at the head and nozzle end of the grain and the grain erosive burning is accounted for. The typical pressure time profile can be divided into three phases; the initial pressure rise, the quasi-steady state phase, and the exhaust phase. These phases are illustrated schematically in Figure 1.

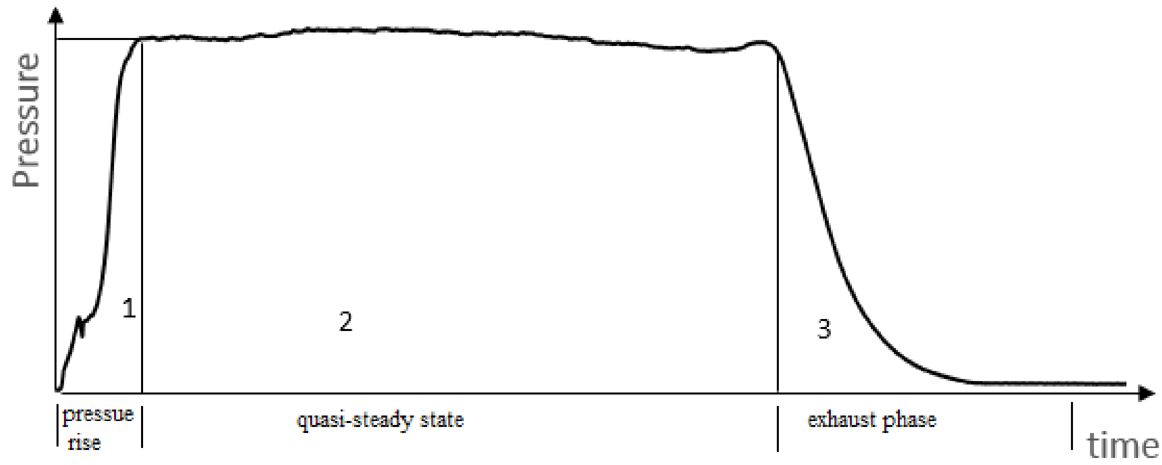

Figure 1: Pressure time profile phases

In the initial pressure rise (ignition) phase, the igniter is activated to bring the chamber pressure to a level sufficient to ignite the propellant grain surface. The initial pressure rise is dependent on the igniter charge rather than the main propellant grain. It is thus overlooked in the model. The Quasi steady state operation phase generally occupies the longest time in the motor operation. In the present analysis, this phase starts directly after ignition. The phase ends at the moment when the burning gases reach the inner wall of the combustion chamber for star perforated grains, this phase is divided into two regimes. The first regime is till the star leg is ended while the second ends when the web is finished. The prediction of pressure history is performed according to the following procedures.
A grain burn-back analysis is performed through analytical method to calculate the burning and port areas of star grain configuration. The gas Mach number at the nozzle end of the grain is evaluated (iteratively) by the following equation;

$$M_n = \frac{A^*}{A_p}\left[\frac{2}{\gamma+1}\left(1+\frac{\gamma-1}{2}M_n^2\right)\right]^{\frac{\gamma+1}{2(\gamma-1)}} \tag{1}$$

where γ, A_p, A^* are Specific heat ratio of the combustion gases, port area of star grain at each burning step and critical section area of the nozzle, respectively. The flow velocity of gases at the nozzle end is then estimated as follows:

$$V_n = \sqrt{\gamma}C^*\Gamma M_n\left(1+\frac{\gamma-1}{2}M_n^2\right)^{\frac{-1}{2}} \tag{2}$$

where Γ, C^* are specific gas constant and characteristic velocity of the propellant, respectively. The stagnation pressure of flowing gases is estimated from the relation:

$$P_{on} = \left[a\rho_p C^* A_b/A^*\right]^{\frac{1}{1-n}} \tag{3}$$

where ρ_p, A_b, n are propellant density, burning area of the grain at each step and the pressure exponent of the propellant, respectively. Hence, the pressure at nozzle end is:

$$P_n = P_{on}\left(1+\frac{\gamma-1}{2}M_n^2\right)^{\frac{-\gamma}{\gamma-1}} \tag{4}$$

Now, the rate of discharge of gases is calculated as:

$$\dot{m}_D = \frac{A^* P_{on}}{C^*} \tag{5}$$

Hence the gas pressure at head end of the grain is:

$$P_h = P_n + \frac{\dot{m}_D V_n}{A_p} \tag{6}$$

The burning rate at the head end of the grain can be obtained by:

$$r_h = aP_h^n \tag{7}$$

where a is the burning rate coefficient. The total burning rate at the nozzle end due to applying the erosive burning rate is:

$$r_n = aP_h^n + \alpha\left(\dot{m}_D/A_p\right)^{0.8} L^{-0.2} e^{(-\beta r \rho_p A_p/\dot{m}_D)} \tag{8}$$

where α, L, β are step regression factor, grain length and head end regression factor. The rate of generation of gases is estimated using the following equation:

$$\dot{m}_G = A_b \rho_p r_{av} \tag{9}$$

where $r_{av} = \frac{r_h + r_n}{2}$

The discharge mass flow rate is obtained more accurately (iteratively) through the following equations:

$$\dot{m}_D \doteq m_G - \frac{\bar{r}_{av}}{r^2 * c^{*2}}\left(\bar{P}_{av}\,\bar{A}_b + V_c\frac{dP}{dy}\right) \tag{10}$$

where: $V_c = V_{ci} + \sum_j \Delta\, y_i \bar{A}_{bj}$

V_{ci} and j are the initial volume of combustion chamber and the burning step, respectively. The rate of change of chamber pressure (dP/dy) is computed as follows:

$$\frac{dP}{dy} = \frac{\bar{P}_{av}}{\bar{r}_{av}}\frac{\Delta r_{av}}{\Delta y} + \frac{\bar{P}_{av}}{\bar{A}_b}\frac{\Delta A_b}{\Delta y} \tag{11}$$

During the quasi-steady state phase, the chamber pressure varies due to the change in the grain surface. The computation of the pressure time curve requires iteration because the burning surface is a function of the distance burnt $\Delta\, y$ during a time increment Δt. The grain web is divided into equal distances $\Delta\, y$. Hence the time increment for the calculations is:

$$\Delta t = \frac{\Delta y}{r_{av}} \tag{12}$$

Finally, during tail off, the burning surface decreases sharply in two distinct regimes. In the first regime, the mass of gases produced by combustion still represents a fraction of flow discharge through the nozzle. In the second regime, after the burning is completed, the remainder of combustion gases is simply exhausting out of the nozzle. The first regime characterized by high port area in the nozzle end section together with a reduced mass flow rate in consequence of reduced burning surface. The conditions of reduced gas velocity and absence of erosive burning (hence, absence of pressure gradient along the chamber) are thus assumed. This can be formatted as follows:

$$P_h = P_n = P_{on} \tag{13}$$

Hence: $r_h = r_n$. The rate of change of chamber pressure is obtained from:

$$\frac{dP}{dy} = \frac{P_{on}}{(1-n)\bar{A}_b}\frac{\Delta A_b}{\Delta y} \tag{14}$$

The second regime is characterized by: (1) zero burning surface and (2) the rate at which the chamber pressure decreases with time is relatively high. The pressure is computed from the relation:

$$P_{on} = P_D \exp[-r^2 c^* A^* (t - t_D)/V_{cf}] \tag{15}$$

where V_{cf}, P_D are the final free volume of the combustion chamber and the discharge pressure, respectively. The discharge mass flow rate can be obtained from:

$$\dot{m}_D = \frac{P_c A_{cr}}{C^*} = \dot{m}_G - \frac{d}{dt}\rho V = \frac{-V}{RT}\frac{dP}{dt} \tag{16}$$

Nozzle critical section erosion is typical in many cases and can significantly impact the value of chamber pressure. The developed model account for nozzle erosion in critical section where the critical diameter expands with time due to erosion expressed by factor (E_r) according to the relation [13]:

$$d_{cr} = d_{cri} + \left(2 * er_{rate}(t - t_{delay})\right) \tag{17}$$

where d_{cr} and d_{cri} are instantaneous and initial critical diameters, respectively. er_{rate} is the erosion rate, and t_{delay} is the time lag between motor ignition and nozzle throat erosion onset.

2.2 Internal ballistics prediction model

A grain with star perforation geometry used designed and tested by Maklad [16] in a standard test motor. Results of this static test are adopted here to validate the performance prediction program. Figure 2 shows the star grain geometry. Table 1 lists the parameters of the grain and the test motor whereas Figure 3 illustrates the measured pressure-time profile of the test case.

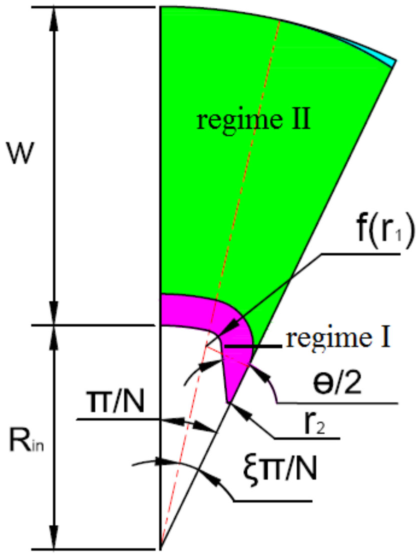

Figure 2: star grain parameters

Table 1 Case study parameters

Propellant characteristics	symbol	value	unit
Propellant characteristic velocity	C^*	1560	m/s
Pressure exponent	n	0.42	---
Burning rate coefficient	a	0.0000113	---
Density of the burning propellant	ρ	1680	Kg/m^3
Specific heat ratio of the combustion gases	γ	1.24	---
Motor characteristics			
Initial critical diameter of nozzle	d_{cr}	0.036	m
Initial free volume of the combustion chamber	V_{ci}	0.004286	m^3
Final chamber volume	V_{cf}	0.017356	m^3
Star grain parameters			
No of star points	N	7	---
Star point angle	θ	74	degree
Angle fraction	ε	0.5058	---
Grain inner radius	R_{in}	0.0235	m
Fillet radius	f	0.0016	m
Web thickness	w	0.0335	m
Length of star grain	L_g	1.6041	m

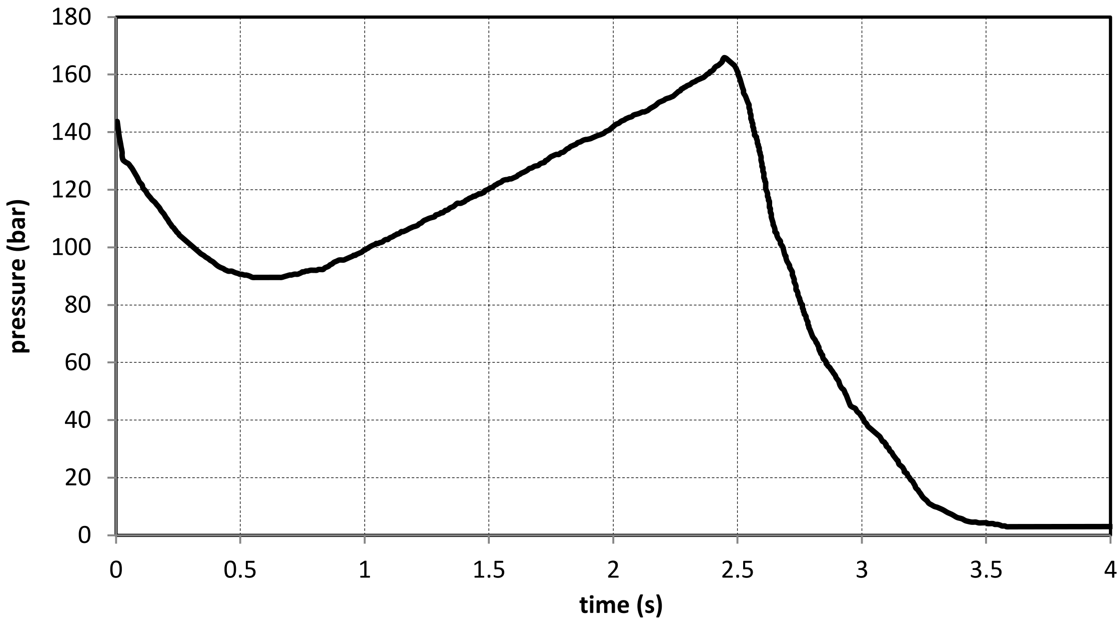

Figure 3: Measured pressure-time profile [14]

2.3 Optimization methods

The developed prediction model involves uncertainties in the given ballistic parameters of the propellant. Six parameters are considered hence namely; burning rate coefficient, a, pressure exponent, n, step regression factor, $\propto$, head end regression factor, β, erosion rate of nozzle critical section, er_{rate}, and delay time for the onset of erosion, t_{delay}. The prediction accuracy of the model is thus dependent on the values of these parameters. The set of values of these parameters that maximize the model accuracy are attained by optimization. The six parameters in concern are allowed to vary within their respectable ranges according to the table below. The values for a and n are arbitrarily chosen to engulf the baseline values provided by the experimental work [16]. Values of other parameters are specified based on previous experience of the authors [13].

Table 1 Ranges of variation of grain and motor parameters in concern

Design parameters	Symbols	Lower Bound	Upper Bound
Burning rate coefficient	a	100e-07	120 e-07
Pressure exponent	n	0.41	0.43
Step regression factor	$\propto$	295e-07	315 e-07
Head end regression factor	β	140	160
Erosion rate of nozzle critical section	er_{rate}	1e-04	3 e-04
Delay time until begin of erosion	t_{delay}	0.01	0.9

A hybrid optimization technique is used to get the minimum RMSE between the theoretical and experimental pressure time profile using Genetic algorithm [17] globally and simulated annealing [18] locally. Genetic Algorithms, GAs, [17] are based on the principle of genetics and natural selection. Here, a "population" is chosen randomly, the fitness of each individual is determined. The operations of selection, crossover, and mutation are used to create the next generation. Simulated Annealing (SA) [18] method simulates the natural process of very slow cooling of heated solids in which the crystalline structures seek the minimum energy path towards solidification. The RMSE is calculated during the quasi-steady state phase only. The optimization is conducted using MATLAB toolbox [19].

3 RESULTS AND DISCUSSION

Figure holds a comparison between the experimental and predicted pressure time profiles of the star perforated grain in concern.

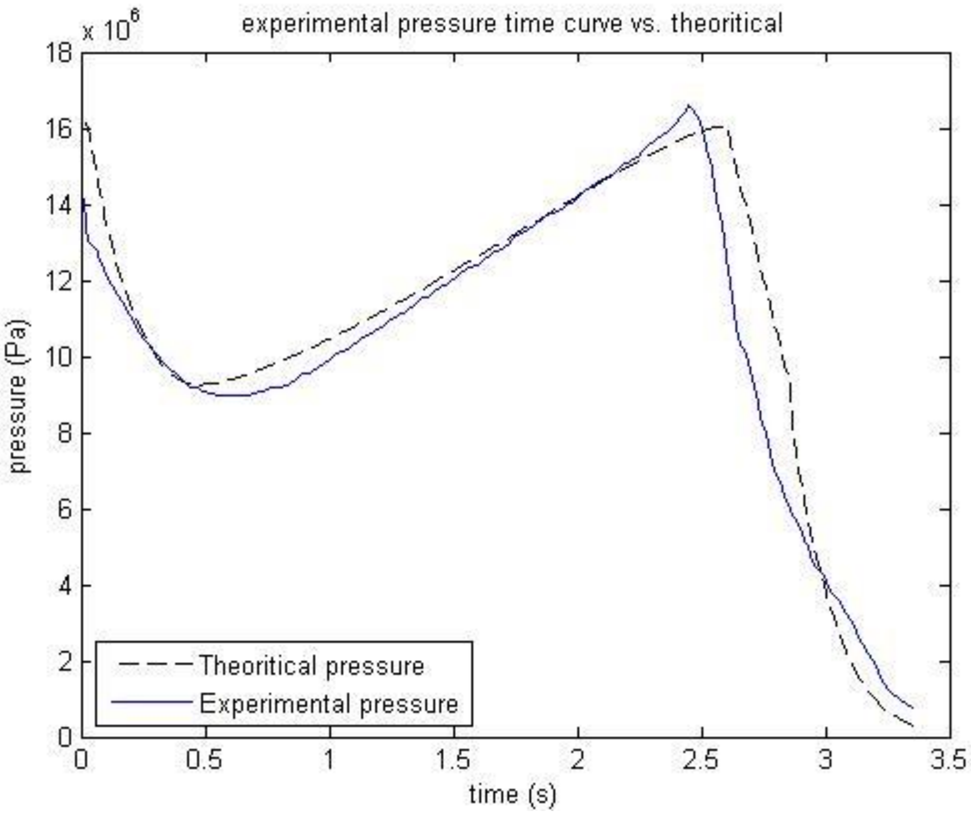

Figure 4: Theoretical and experimental pressure-time profiles

Generally, prediction tool manages to predict the trend of pressure-time profile. However, the theoretical model overestimates the starting pressure value and the pressure drop rate during the starting regressive burning phase. This may indicate an overestimation of the initial burning surface area of the star perforation. The model also overestimates the steady-state phase duration. The overall root mean square of prediction during the steady-state phase only (enduring for about 2.5 seconds) is 6.5%.

Next, the optimization algorithm is applied. Figure show the convergence history of genetic algorithm optimizer. The solution was found to converge after 200 iterations. The RMSE of prediction during the steady-state phase is improved to 2.38 %. Optimization is then continued using Simulated Annealing. Figure shows the function value convergence during the simulated annealing optimization. The solution is found to converge after 3245 iterations and the RMSE is improved during the steady-state phase to 2.36 %. The slight improvement in the SA optimization phase indicates that GA has reached the global optimum solution is a high accuracy.

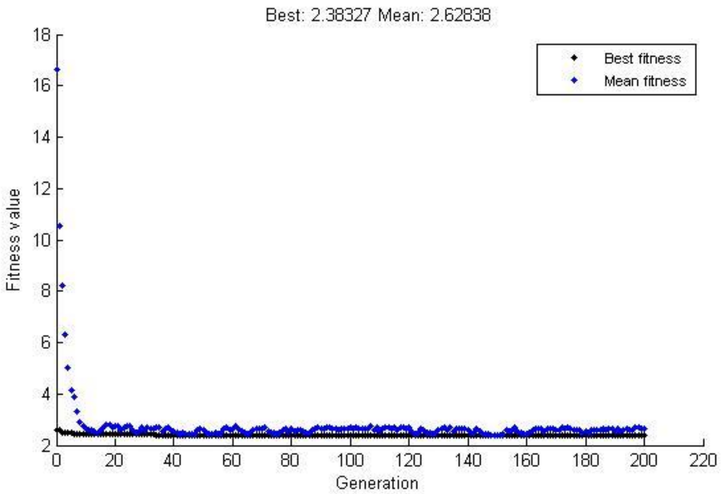

Figure 5: Convergence history of GA optimization

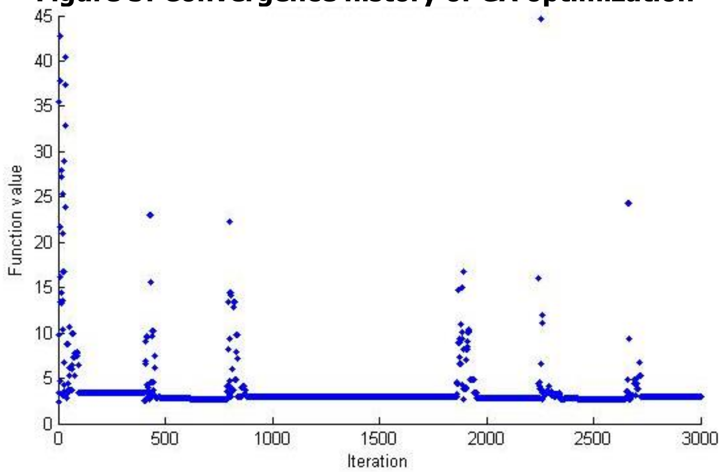

Figure 6: Convergence history of SA optimization

Figure 7 shows the optimized pressure-time profile. The improvement in prediction accuracy is evident especially in the starting regressive burning phase.

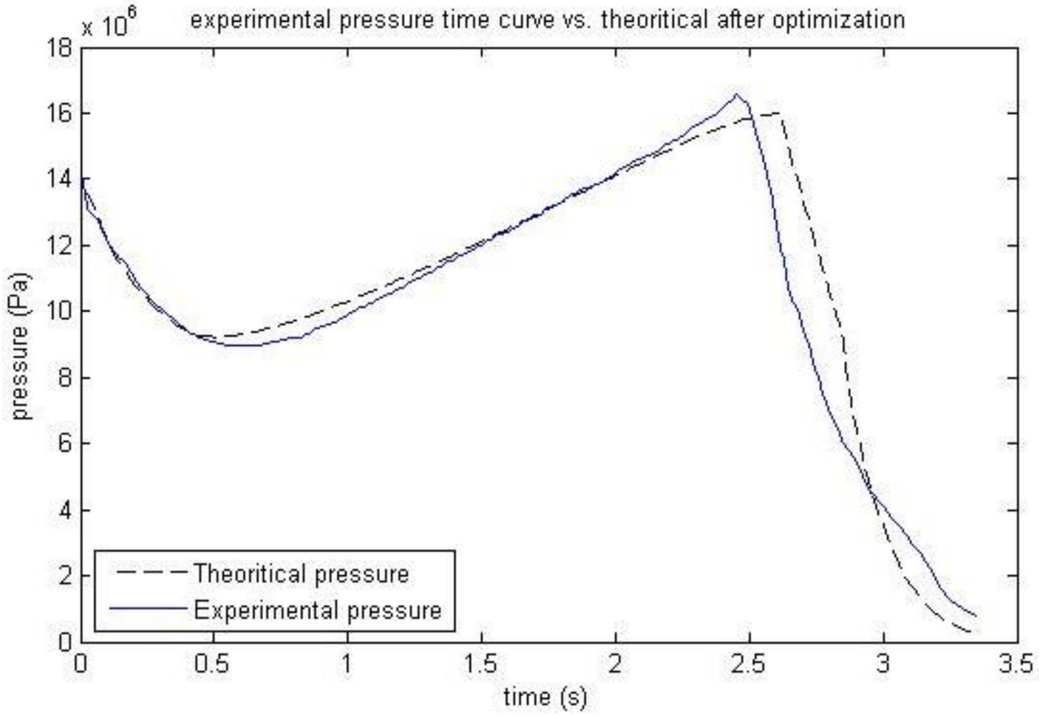

Figure 7: Pressure time curve after optimization

Table 2 below lists the optimized values of the parameters in concern in this study. For the sake of comparison, the corresponding baseline values, lower and upper bounds of variation are also listed.

Table 2 Design parameters at all design phases and lower and upper bounds.

Design parameters	Symbols	Lower Bound	Upper Bound	Base line values	Optimized solution GA	Optimized solution SA
Burning rate coefficient	a	100e-07	120 e-07	113e-07	110.13 e-07	110.12 e-07
Pressure exponent	n	0.41	0.43	0.42	0.422	0.421
Step regression factor	$\propto$	295e-07	315 e-07	308e-07	304.91 e-07	304.81 e-07
Head end regression factor	β	140	160	150	154.909	154.859
Erosion rate of nozzle critical section	er_{rate}	1e-04	3 e-04	2e-04	1.053 e-04	1.049 e-04
Delay time until begin of erosion	t_{delay}	0.01	0.9	0.7	0.0256	0.0254
Root mean square error of prediction	RMSE	-	-	6.5 %	2.38 %	2.36 %

4 CONCLUSIONS AND FUTURE WORK

A mathematical model is developed to predict the pressure-time profile of a star-perforated solid propellant grain. The developed tool is capable of predicting the performance of a test case that was experimentally tested with a reasonable accuracy. The prediction accuracy of the model is enhanced by tuning the grain ballistic and geometric parameters using a hybrid GA/SA. Upon performing the hybrid optimization technique, the prediction model tool becomes more accurate. Further work should focus on improving the prediction accuracy of the model during the exhaust phase. The developed technique can be alsoutilized in predicting of grain geometry to satisfy a predefined performance. The model can be enhanced by incorporating different grain geometries.

REFERENCES

1. G. Puskulcu; 2004; "Analysis of 3-D Grain Burnback of Solid Propellant Rocket Motors and Verification with Rocket Motor Tests"; *MS. Thesis*; Dept. of Mechanical Engineering; METU.
2. K. Nisar, L. Guozhu, and Q. Zeeshan; 2008; "A hybrid optimization approach for SRM finocyl grain design"; *Chinese Journal of Aeronautics;* **21**; pp. 481-487.
3. F. M. Villanueva, L. S. He, and D. J. Xu; 2014; "Solid Rocket Motor Design Optimization Using Genetic Algorithm"; *Advanced Materials Research*; **509**; pp. 502-506.
4. A. Kamran, L. Guozhu, A. F. Rafique, S. Naz, and Q. Zeeshan; 2010; "Star Grain Optimization using Genetic Algorithm"; in *51st AIAA/ASME/ASCE/AHS/ASC Structures, Structural Dynamics, and Materials Conference 18th AIAA/ASME/AHS Adaptive Structures Conference 12th;* pp. 3084.
5. A. Kamran and L. Guozhu; 2010; "Design and optimization of 3D radial slot grain configuration"; *Chinese Journal of Aeronautics;* **23**; pp. 409-414.
6. M. A. Raza and W. Liang; 2013; "Design and Optimization of 3D Wagon Wheel Grain for Dual Thrust Solid Rocket Motors"; *Propellants, Explosives, Pyrotechnics;* **38**; pp. 67-74.
7. M. A. Raza and W. Liang; 2012; "Robust performance optimization of dual thrust rocket motor"; *Aircraft Engineering and Aerospace Technology;* **84**; pp. 244-251.
8. M. A. Raza and W. Liang; 2011; "Robust Design Optimization of an Aerospace Vehicle Prolusion System"; *Mathematical Problems in Engineering;* **2011**.
9. M. Aamir Raza and W. Liang; 2012 ; "Robust Design Optimization of Dual Thrust Solid Propellant Motors due to Burning Rate Uncertainties"; *Propellants, Explosives, Pyrotechnics;* **37**; pp. 476-488.
10. O. Yucel, S. Acik, K. A. Toker, Z. Dursunkaya, and M. H. Aksel; 2015; "Three-dimensional grain design optimization of solid rocket motors"; in *Recent Advances in Space Technologies (RAST), 7th International Conference on;* pp. 471-476.
11. S. Acik; 2010; "Internal Ballistic Design Optimization of a Solid Rocket Motor"; *Master Thesis*; Mechanical Engineering; Middle East Technical University; Turkey.
12. R. H. Sforzini; 1980; "An automated approach to design of solid rockets utilizing a special internal ballistics model"; *AIAA*.
13. A. R. A. Gawad, M. Y. Ahmed, H. M. Abdalla, and M. A. El-Senbawy; 2016; "Pressure Profile Prediction of Dual-Thrust Rocket Motors under Uncertainties"; *Propellants, Explosives, Pyrotechnics;* **41**; pp. 965-971.
14. M. Barrere; 1960; "*Rocket Propulsion"*.
15. G. P. Sutton and O. Biblarz; 2010; "*Rocket Propulsion Elements*".
16. A. Maklad; 1994; "Design Optimization of Solid Rocket Motors"; *Master Thesis*, MTC.
17. D. E. Goldberg; 1989; "Genetic Algorithms in Search, Optimization, and Machine Learning, 1st ed "; Addison–Wesley, Reading, MA.
18. S. Kirkpatrick, C. D. Gelatt, M. P. Vecchi; 1983; "Optimization by Simulated Annealing"; Science; 220 (4598), pp: 671-680.
19. M. Abramson; 2004; "Genetic Algorithm and Direct Search Toolbox User's Guide For Use with MATLAB"; *The MathWorks*.